Original Research Article

HOP-DERIVED XANTHOHUMOL INDUCES HL-60 LEUKEMIA CELLS DEATH

Abstract

Background. Acute promyelocytic leukemia (APL) affects both kids and adults, however it is more prevalent in younger population. Although APL has a favorable prognostic, patients that do relapse often do not favorable respond to additional chemotherapy. Therefore, there is a need to further identify ways to overcome these challenges.
Hypothesis: In this study, we examined antileukemic effects of xanthohumol, a prenylated flavonoid derived from hops (Humulus lupulus), on human promyelocytic HL-60 cells.
Materials and Methods. HL-60 cells were exposed to different concentrations of xanthohumol (μM) for 24 h. Cell viability, cell morphology, chromatin condensation, cPARP-1 level, and caspase-3 activation, and the expression of $p21^{WAF1/Cip1}$ were analyzed.
Results. Xanthohumol reduced HL-60 cell viability in a dose-dependent manner. Xanthohumol induced a dose-dependent profound morphological changes including cell shrinkage and blebbing, and significantly increased the number of cells with condensed chromatin. Xanthohumol significantly increased the level of cPARP-1, active caspase-3, and the expression of $^{p21WAF/CIP}$ mRNA.
Conclusion. These data indicate that xanthohumol induces HL-60 cells death by regulating cell cycle progression and apoptosis. This study suggests that xanthohumol may have antileukemic preventive effects.

Key words: Acute promyelocytic leukemia, apoptosis, caspase-3, p21, xanthohumol, plant derived, HL-60 cells

Abbreviations

APL acute premyelocytic leukemia

PARP-1 polymerase associated reactive protein 1

cPARP-1 cleaved PARP-1

FBS Fetal Bovine Serum

XN xanthohumol

Introduction

Acute promyelocytic leukemia (APL) a subtype of acute myeloid leukemia (AML) represents 5-20% of AML. Each year ~ 600-800 new cases of leukemia are diagnosed in the USA [1]. Although APL has a good prognosis, if untreated or if the disease relapses, the mortality rate is high [2]. Approximately, 30% of patients relapse [3]. Epidemiologic studies show that APL is more common in children and young adult patients and among Hispanics [4]. Although new therapeutic approaches have been developed, APL still remains an aggressive subtype of AML and with high rates of early death [5-6]. Indeed, approximately 17.3% of cases undergo early death within one month of diagnosis due to severe hemorrhages [7]. Therefore, finding new approaches to improve APL treatment outcome is of great importance. Plant-based compounds alone or in combination with chemodrugs have been shown to have antitumor effects and to improve treatment outcome of several malignant hematologies including Hodgkin's disease and acute lymphoblastic leukemia [8-11]. For example, plant-derived alkaloids vincristine and vinblastine are approved for the treatment of hematological malignancies and other cancers [10-11]. Vincristine is used to treat childhood leukemia whereas vinblastine is used in combination with chemodrugs to treat breast and bladder cancers [12-14]. Although vincristine is successful for childhood leukemia often leads to neuropathy 14-15]. Thus identifying plant compounds with antileukimic properties and less toxicity will contribute to improve treatment outcome [11, 16-17]). Plant-derived prenylated flavonoid, xanthohumol

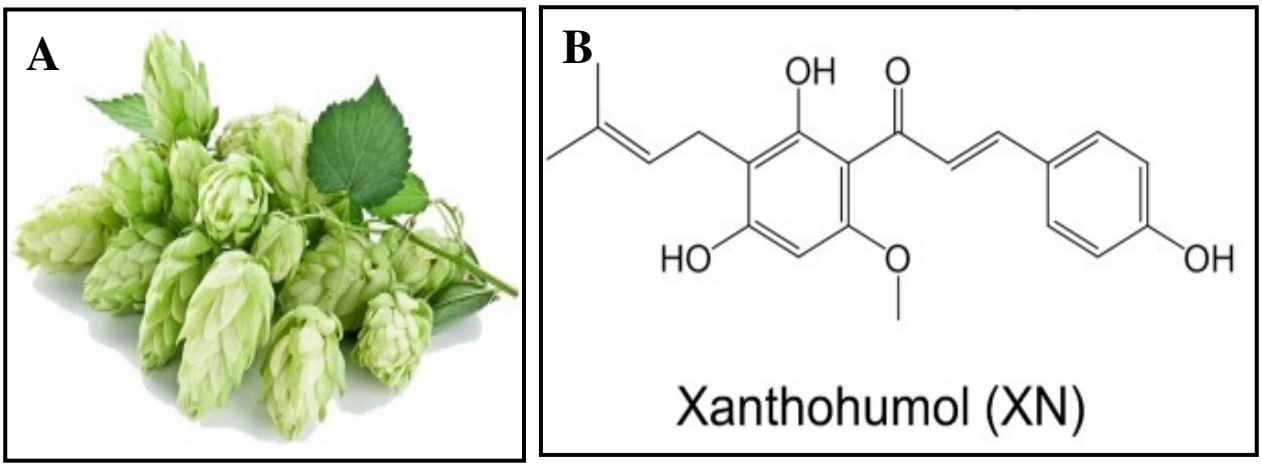

(XN), has been shown to have biological properties. Xanthohumol is present in the cones of hop plant (*Humulus lupulus* L.) Fig. 1 [18].

Figure 1. Hop plant cone (Humulus lupulus L) (A), and xanthohumol chemical structure (B). Xanthohumol is a prenylated chalcone found in the cone of hop plant [18].

In hops, xanthohumol content vary from 0.1% to 1% dry weight [19]. In addition of being used in brewing industry, numerous studies also showed xanthohumol's numerous biological effects including anti-inflammatory, anti-oxidant, and anti-infectious [20-23]. Recent studies showed xanthohumol increased lipid and glucose metabolism [24-26]. Xanthohumol anti-carcinogenic properties have been shown on many different cancer cell types including liver, prostate, endometrial, colon, and lung [26-31]. The exact mechanism by which xanthohumol exerts its effects is not fully understood, however studies suggest that it inhibits cell proliferation and induces apoptosis by upregulating p53 and inducing S phase cell cycle control genes [31-32].

While xanthohumol anti-carcinogenic effects were studied on many cancer cell types, fewer studies examined xanthohumol effects on human acute promyelocytic leukemia. In the present study, we examined xanthohumol effects on acute promyelocytic leukemia HL-60 cells.

Materials and Methods

Chemicals. Xanthohumol was purchased from Sigma Aldrich (Saint Louis, MO). Caspase-3 assay kit was purchased from Thermofisher Scientific/Invitrogen (Waltham, MA), MTT assays was purchased from Promega (Madison, WI), and Hoechst 33258 was purchased form Thermofisher Scientific/Molecular Probes, whereas PARP-1 antibody was purchased from Cell Signaling Technologies (Danvers, MS).

Xanthohumol preparation. Xanthohumol was prepared in DMSO according to the methods previously described [27]. A stock solution (50 mM) of xanthohumol was prepared and kept at -20°C and used within 2-3 weeks. For cell culture studies, xanthohumol stock solution was further diluted to various concentrations in the basal media before cell treatment thus achieving a final concentration of 0.1% DMSO.

Cell culture. Human acute promyelocytic leukemia HL-60 cell line was purchased from the American Type Culture Collection (ATCC, Manassas, VA). HL-60 cells were cultured in Iscove's Modified Dulbecco's Medium (IMDM) supplemented with penicillin, streptomycin, L-glutamine and 20% fetal bovine serum. The cells were cultured at 37˚C in humidified incubator with 95% air and 5% CO2.

Cell viability. Cell viability was measured using Celltiter 96 Aqueous One Solution Cell Proliferation Assay according to the protocol provided by the manufacturer (Promega Inc, Madison, USA). Briefly, this assay contains tetrazolium compound (3-(4,5-dimethylthiazol-2-yl)-5-(3-carboxymethoxyphenul)-2-(4-sulfophenyl)-2H-tetrazolium salts; MTS) and an electron coupling reagent (phenazine ethosulfate; PES). The MTS tetrazolium compound is reduced by

cells into a colored formazan product that is soluble. The cells were subcultured in 96-well plates at a density of 10,000 cell/well in 5% FBS/DMEM/Penicillin/Streptomycin (10,000/1000 units) for 24 h at 37ºC/5% CO_2. After 24 h, the cells were treated with xanthohumol at 6.25, 12.5, 25, and 50 µM for 24 h. After 24 h of treatment, 20 µl of tetrazolium were added to the cells and incubated for 4 h at 37ºC/5%CO_2. After 4 h, 25 µl of 10% SDS were added and the plate was incubated for 18 h at room temperature in a humidified container. After 18 h, the absorbance was measure at 490 nm using a 96-well microplate reader (SpectraMax 190, Molecular Scientifics, NH).

RNA isolation. Total RNA was extracted using Trizol® (Invitrogen, CA) according to the manufacturer's protocol. To ensure a good RNA quality, the integrity and quality of the total RNA was evaluated using 28S/18S ratio and a visual image of the 28S and 18S bands were evaluated on the 2100 Bioanalyzer (Agilent Technologies, Santa Clara, CA). Concentration of the total RNA was assessed using the NanoDrop-1000 Spectrophotometer (NanoDrop Technologies, Germany).

Quantitative real-time (q)PCR. qPCR for target genes was determined using total RNA and cDNA was generated using a High-Capacity cDNA Reverse Transcription kit and TaqMan gene expression assays (Applied Biosystems Inc., CA). The levels of p21 and 18S mRNA was measured using SYBR-Green Master mix and gene specific primers according to manufacturer's protocol (Applied Biosystems Inc.). All qRT-PCR reactions were performed on 7500 instrument (Applied Biosystems Inc.). In the qRT-PCR analysis of genes, the dissociation curve showed the absence of a secondary peak, indicating no presence of primer dimer. The expression level of each gene was determined by following formulas: fold change = $2-\Delta\Delta Ct$, where ΔCt (cycle

threshold) = $Ct_{target\ gene}$ - $Ct_{endogenous\ control\ gene}$, and $\Delta\Delta Ct = \Delta Ct_{treated\ sample} - \Delta Ct_{control\ sample}$. 18S was used as an endogenous control gene [33-34].

Western blot. After treatments, the cells were lysed in 1X SDS lysis buffer (50 mM Tris-HCl, pH 6.8, 2% SDS, 10% glycerol). Total protein was quantified by the BCA method. β-mercaptoethanol was added to lysates to a final concentration 100 mM. Equal amounts of total protein were separated by 4-12% SDS-PAGE and transferred to a PVDF membrane. Membranes were blocked with 5% non-fat milk in 1X PBS containing 0.05% Tween-20 for 1 h at room temperature. Membranes were then incubated with PARP-1 primary antibody (Cell Signaling Technologies) at 4ºC overnight. After the incubation the membranes were washed three times in 1X PBS with 0.05% Tween-20 for 10 min and then incubated for 1 h at room temperature with horseradish peroxidase (HRP) conjugated goat anti-mouse IgG in 5% non-fat milk/1X PBS/ 0.05% Tween-20. Membranes were then washed five times for 10 min in 1X PBS with 0.05% Tween-20 and the proteins were visualized using an ECL Chemiluminescence Kit (Millipore, MA). Relative protein level was determined after normalization to beta-actin.

Cell morphology. The cells were cultured in 6-well plates in 5%FBS/IMDM/Penicillin/Streptomycin for 24 h at 37ºC/5% CO_2. After 24 h, the cells will be treated with xanthohumol 6.25, 12.5, and 25 µM in basal media for 24 h. After 24 h, the cell morphology micrographs were taken using phase-contrast inverted microscopy. Images will be captured using a Carl Zeiss Axiovert 200 microscope equipped with Spot Camera.

Nuclear staining with Hoechst 33258. The cells were seeded on cover slips in 6-well plates and allowed to grow overnight. The cells were treated with various concentrations of xanthohumol for 24 h. At the end of the incubation period, the cells fixed in 10% paraformaldehyde/PBS for 20 min at RT, and the plate spun down at 1000 rmp for 2 min, and washed with cold PBS. The

cells were stained with fluorescent dye Hoechst 33258 (10 µg/ml; Molecular Proves, NY) and incubated for 15 min at RT. The slides were examined and the apoptotic cells were identified according to the condensation and fragmentation of their nuclei observed under Olympus IX70 microscope (Olympus Optical Co., Ltd, Japan) equipped with a Retiga 2000R FAST camera (Qimaging, Canada). Images were acquired using SimplePCI software (Compix Inc., Sewickley, PA).

Human Caspase-3 (active) ELISA assay. The cells were cultured in growth media and after 24 h the media was changed to basal media and xanthohumol was applied for 24 h. After the treatment, the cells were washed, scraped off in 1 X PBS and spun down at 5,000 rpm for 3 min and the pellet was lysed in cell RIPA extraction buffer (Thermofisher Scientific) with 1 mM PMSF, and protease inhibitor (Sigma Aldrich) on ice and sonicated 10 sec on ice, and then centrifuged at 14,000 rpm for 10 min at 4ºC. The samples were further diluted 10X in assay's standards' diluent buffer. Caspase-3 assay was performed according to manufacturer's protocol (Thermofisher Scientific/Invitrogen).

Statistical analysis. Data are presented as mean ± SEM from three experiments. Statistical analysis was performed using one-way analysis of variance (ANOVA) and Student's paired *t*-test with a significance level of $p \leq 0.05$ versus non-treated control samples.

Results

Xanthohumol effect on cell viability

The effect of xanthohumol on the proliferation of HL-60 cells was determined using MTT assay. The HL-60 cells were treated with 6.25, 12.5, 25, or 50 µM of xanthohumol for 24 h (Figure 2). Xanthohumol significantly decreased HL-60 cells viability at 12.5, 25, and 50 µM compared to control ($p < 0.05$, Figure 2).

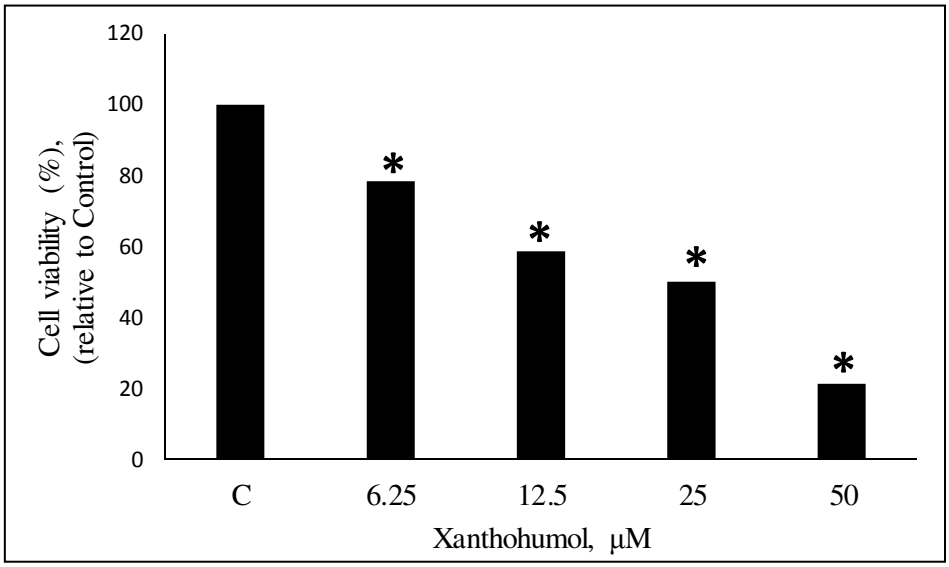

Figure 2. The effect of xanthohumol on the viability of HL-60 cells. The cells were treated with 6.25, 12.5, 25, and 50 μM of xanthohumol for 24 h. Cell viability was measured using Cell Titer 96 Aqueous One Solution Assay as described in Materials and Methods. Data is presented at % cell viability relative to control, n = 3, * Statistical significance, ANOVA, $p < 0.05$, vs control.

Xanthohumol effect on cell morphology

The effect of different concentrations of xanthohumol on cell morphology were analyzed using light microscopy. At 6.25 μM, xanthohumol did not induce profound cell morphology changes compared to control cells, although some cells displayed vesicles and mild shrinkage (Figure 3, arrow). At concentrations higher than 6.25 μM, xanthohumol induced strong cell morphological changes such as cell-size shrinking and rounding, and formation of cytoplasmic visible vesicles (Figure 3, dashed arrow). At the highest tested concentration of 25 μM, xanthohumol induced profound cell rounding, shrinking, and a reduction in cell number (Figure 3, arrow and dashed arrow).

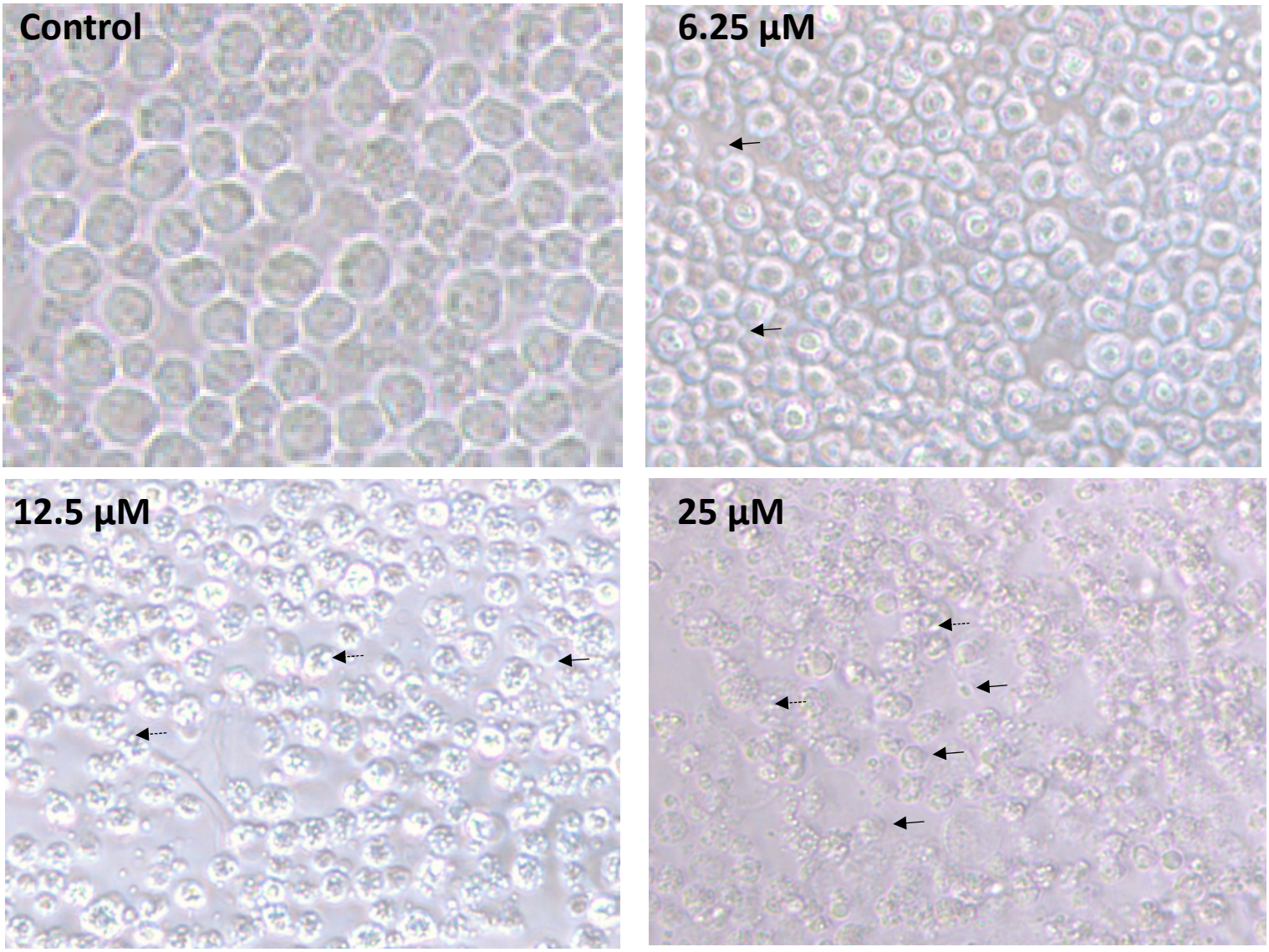

Figure 3. Cell morphology changes in the absence and presence of xanthohumol. The cells were seeded in 5% FBS growth media for 24 h followed by xanthohumol treatment with different concentrations (µM) as shown in the figure for 24 h. Representative micrographs of one experiment are shown, n = 3. The micrographs were recorded using an inverted phase-contrast light microscope. Arrow= cell shrinkage and blebbing, dotted arrow = reduced cell density.

Xanthohumol effect on nuclear chromatin

The effect of xanthohumol on nuclear chromatin was analyzed following treatment of cells with different concentrations of xanthohumol (Figure 4). Chromatin changes were determined using

nuclear staining dye, Hoechst 33258, and then the cells were examined using fluorescent microscopy. Cells treated with different concentration of xanthohumol displayed nuclear chromatin changes such as chromatin condensation which fluoresced bright blue (arrow), whereas control cells stained dark blue without bright blue staining and displayed a normal, round and unpunctuated nucleus (Figure 4A). The cells treated with xanthohumol showed condensed and fragmented nuclei which displayed bright blue fluorescent appearance compared with control, and these cells were scored as apoptotic cells (Figure 4A, dashed arrow). Xanthohumol significantly increased the number of apoptotic cells at concentration higher than 6.25 μM compared to control (Figure 4B). The number of apoptotic cells was significantly higher when the cells were treated with 12.5, 25, or 37.5 μM of xanthohumol having a 21-, 40.5

A

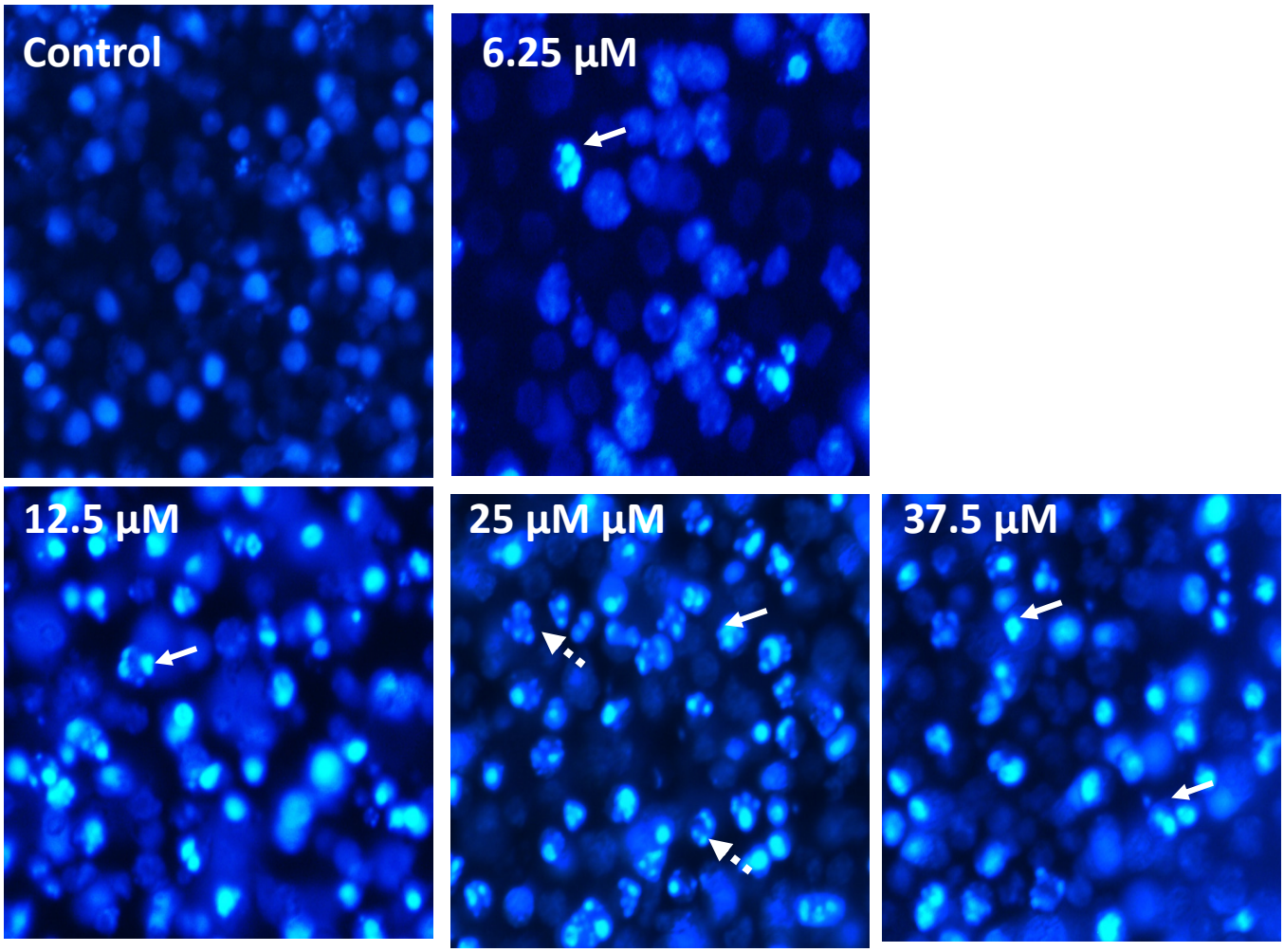

and 42.2-fold increase in the number of apoptotic cells compared to control, respectively ($p < 0.05$, Figure 4B).

B

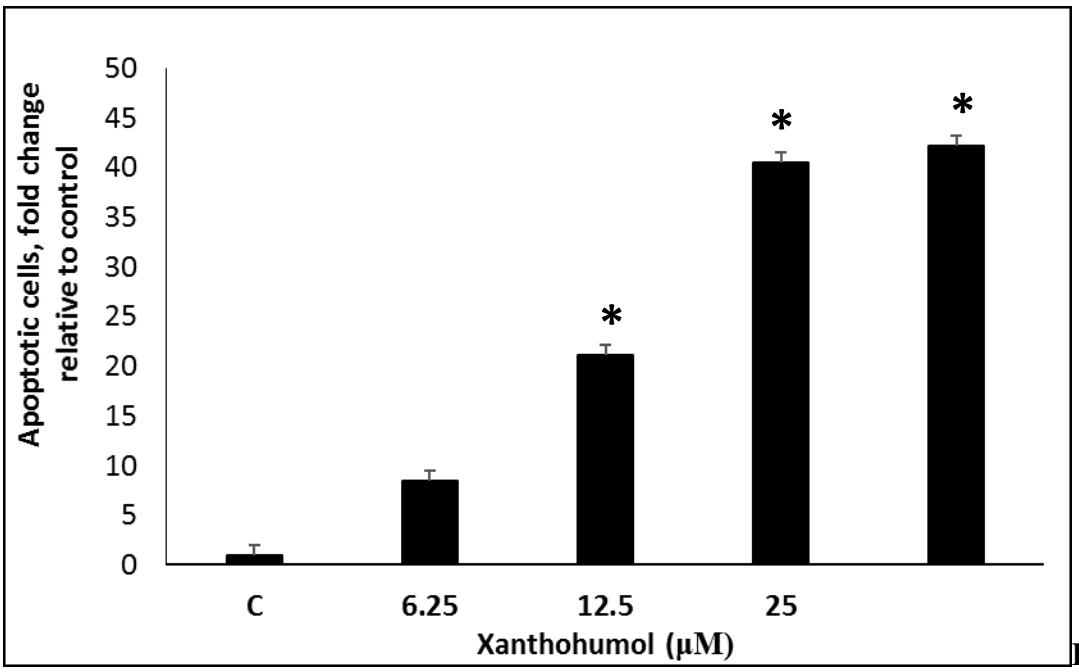

Figure 4. The effect of xanthohumol on nuclear morphology. The cells were cultured on cover slips in 5% FBS growth media for 24 h then treated with different concentrations of xanthohumol (µM) as shown in the figure. After the treatment, the cells were stained with Hoechst 33258 and analyzed as described in Materials and Methods. A) The micrographs were taken with a fluorescent microscope. One representative micrograph is shown, n = 3. The arrow indicates condensed chromatin and condensed nuclei and were counted as apoptotic cells; punctuated nuclei= dotted arrow. B) The percentage of apoptotic cells relative to control. The values are the mean of two independent experiments, with 100 cells counted under each condition and experiment. * Statistically significant, ANOVA, $p < 0.05$ vs control.

Xanthohumol induces PARP-1 cleavage

To identify which pathway of apoptosis xanthohumol activates, we analyzed PARP-1 cleavage (cPARP-1). The cells were treated with 6.25 or 12.5 µM of xanthohumol and cell lysates was subjected to Western blot analysis for PARP-1 cleavage (Figure 5A). cPARP-1 level was significantly increased by both concentrations, 6.25 and 12.5 µM, of xanthohumol compared to control ($p < 0.05$, Figure 5B).

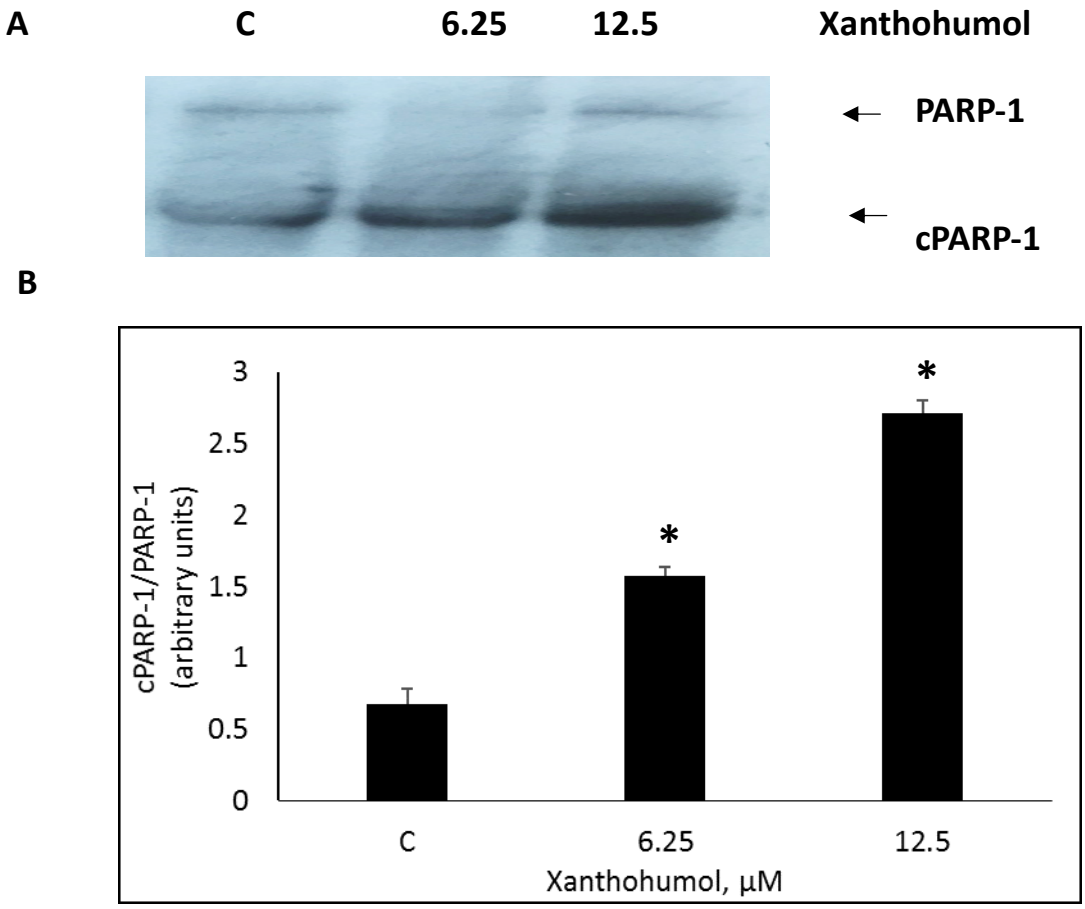

Figure 5. Xanthohumol activates PARP-1. The cells were cultured in 5% FBS growth media for 24 h then treated with 5 and 12.5 µM of xanthohumol for an additional 24 h. After the treatment, the cells were lysed, and the cell lysate was subjected to Western blot analysis as descried in Materials and Methods. One representative blot is shown. B) cPARP-1 quantitative analysis (arbitrary units), n = 3. * Statistically different, ANOVA, $p < 0.05$ vs control.

Xanthohumol activates caspase 3

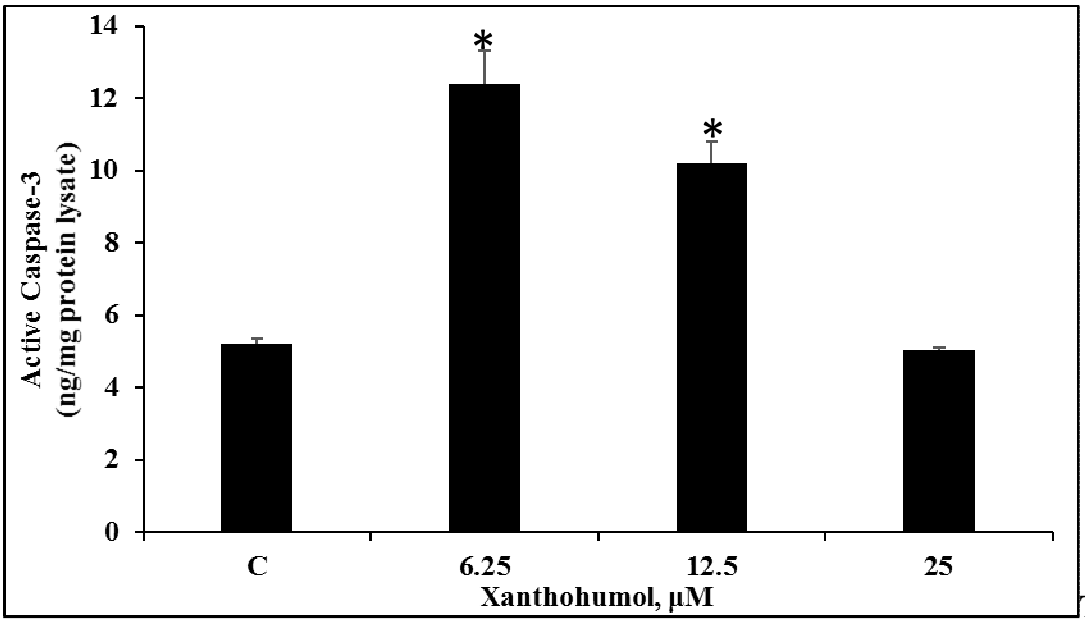

To further investigate the mechanism by which xanthohumol induces HL-60 cytotoxicity, we performed additional experiments to detect active caspase-3. Using active caspase-3 ELISA, the results indicated that HL-60 cells treated with 6.25 or 12.5 µM of xanthohumol had a significant increase in active caspase-3 (Figure 6). In samples treated with 25 µM of xanthohumol, active caspase-3 level was not significantly different compared to control samples (Figure 6).

Figure 6. Xanthohumol activates caspase 3. The cells were cultured in 5% FBS growth media for 24 h and then treated with 6.25, 12.5, and 25 µM of xanthohumol for an additional 24 h. After the treatment, the cells were lysed, and cell lysate was subjected to caspase 3 assay as descried in Materials and Methods. The data represents the mean ± SEM, n = 4. *Statistically significant, ANOVA, $p < 0.05$ vs control.

Xanthohumol effects on p21$^{WAF1/Chip1}$

To further determine the mechanism by which xanthohumol inhibits cell growth, we performed an analysis on cycle control gene p21. Cells treated with 12.5 µM of xanthohumol had 18.3-fold increase of p21 mRNA compared to control (Figure 7).

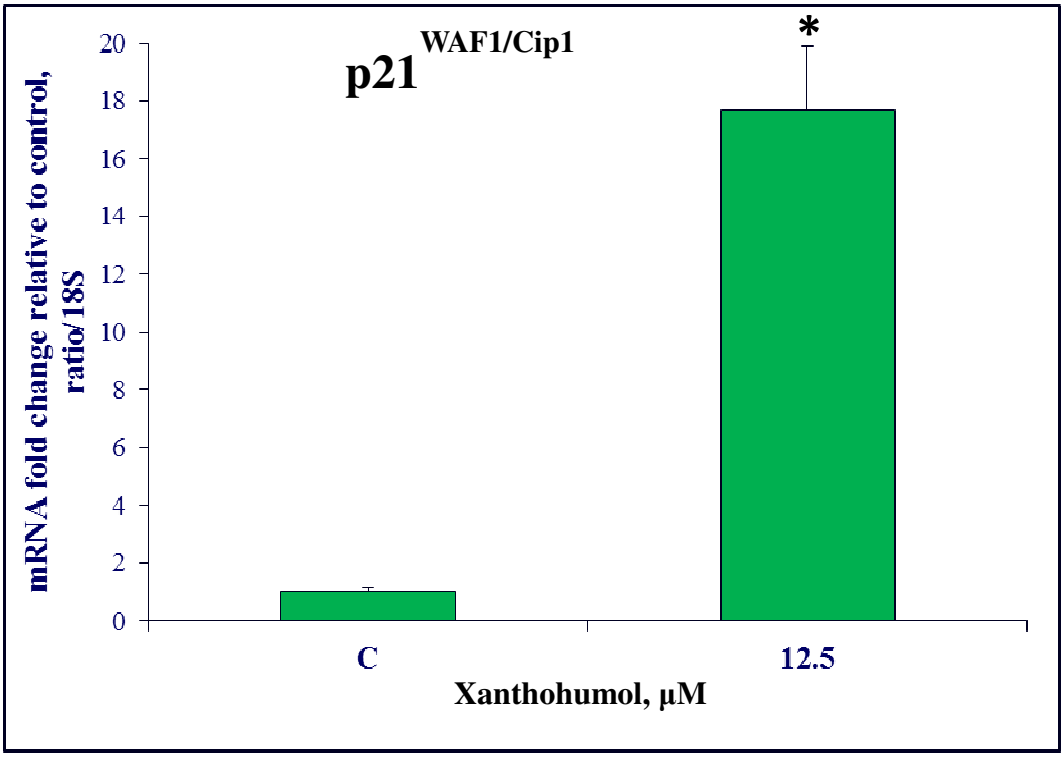

Figure 7. Regulation of $p21^{WAF1/Cip1}$ mRNA in HL-60 cell treated with xanthohumol. The cells were treated with XN 12.5 µM for 24 h and RNA and qPCR were performed as described in Materials and Methods. The data is presented as mRNA fold change relative to 18S. The data represents the mean ± SEM, n = 4. *Statistically significant, ANOVA, *, $p < 0.05$ vs control**.**

Discussion

AML relapse is often observed regardless of the initial cytotoxic effect of traditional chemodrugs [35]. The exact mechanisms of how AML relapses are not fully understood, however it is thought that acquisition of resistance to the initial treatment and accumulation of mutations may contribute to AML relapse [36]. To aid in alleviating less desirable chemotherapy outcome including side effects and chemo-resistance, plant-based natural products are becoming of interest moreover as natural-derived products have guided the development of anti-cancer agents initially. For example, the discovery of paclitaxel in the bark of Pacific yew led to anticancer drug, paclitaxel that is used to treat cancer particularly breast and non-small cell lung cancer [37]. Similarly, vinblastine and vincristine are also the first plant-based alkaloids clinically used

to treat various cancers including leukemia in children. However, both vinblastine and vincristine are often associated with peripheral nerves toxicity [14, 38].

Hop plant cones contain prenylated flavonoids among which xanthohumol have been shown to have cytotoxic effects and to modulate carcinogenesis [39-40]. Numerous studies analyzing biological activity of xanthohumol showed that is antiproliferative and antitumor [41-43]. The mechanisms through which xanthohumol exerts its antitumor properties includes inhibition of alkaline phosphates and upregulation of cell cycle genes in the G0/G1 phase including p21 [40, 43]. In the present study, we show that xanthohumol inhibited HL-60 cell proliferation is a dose-dependent manner, and that at the highest tested dose of 50 μM, only 21% of cell were viable. To further investigate the mechanism involved in the cytotoxic effect of xanthohumol, we analyzed chromatin condensation. We used Hoechst 33258 staining to determine apoptotic cells, and we found that xanthohumol dose-dependently increased the number of apoptotic cells. Xanthohumol induced typical apoptotic nuclear morphology including chromatin condensation and nuclear fragmentation.

Apoptosis is well organized cellular process in a sequence of steps that leads to the elimination of cells under normal physiological conditions. However, in tumor cells apoptosis is an induced process primarily by chemotherapy [44]. In the present study, we examined the mechanism of apoptosis of xanthohumol in HL-60. Xanthohumol significantly increased active capsase-3 by 2.39- and 2-fold compared to control at 6.25 and 12.5 μM, respectively. At 25 μM, caspase-3 was not significantly different from control. Nuclear staining showed that at the same concentrate of 25 μM, 85% pf cells displayed condensed and fragmented chromatin, indicating that at this concentration xanthohumol cytotoxic effect was profound. To further determine xanthohumol apoptotic mechanism, Western blot analysis showed that xanthohumol activated

PARP cleavage. Cleaved PARP is a hallmark of apoptosis [45]. While many caspases cleave PARP-1, caspase-3 has been shown to cleave PARP-1. Our data indicate that xanthohumol increased active caspase-3 at 6.25 μM and increased PARP cleavage at 12.5 μM, thus suggesting that capase-3 activation proceeds PARP cleavage. Soldani et al. [46] monitoring PARP-1 in Hep2 cells found that PARP-1 cleavage takes place after caspases activation and the larger fragment p89 of PARP-1 is detected in the cells undergoing apoptosis and also have profound nuclear fragmentation. To further understand cytotoxic effect of xanthohumol, we investigated its effect on $p21^{WAF1/CIP1}$ mRNA. p21 mRNA was increased 18-folds in cells exposed to 12.5 μM of xanthohumol compared to control. $p21^{WAF1/CIP1}$ is a member of the CDKIs that inhibits G1 cyclin/Cdks thus arresting cell cycle progression in the G1/S phase [47-48]. Additionally, p21 modulates cell apoptosis [48-49].

Conclusions

The present study demonstrates that xanthohumol significantly decreases HL-60 cells viability and induces apoptosis through the activation of PARP-1 and p21 gene that controls cell cycle in the G1/S phase. These results suggest that xanthohumol induces leukemia cells death and warrants potential therapeutic investigation.

References

1. Yamamoto JF, Goodman MT. Patterns of leukemia incidence in the United States by subtype and demographic characteristics, 1997-2002. Cancer Causes Control, 2008, 19:379-90.
2. Elbahesh E, Patel, Tabbara IA. Treatment of acute promyelocytic leukemia. Anticance research, 2014, 34:1507-1517.
3. Huang J, Sun M, Wang Z, Zhang Q, Lou J, Cai Y, Chen W, Du X. Induction treatments for acute promyelocytic leukemia: a network meta-analysis. Oncotarget, 2016, 7:71974–71986.
4. Dores GM, Devesa SS, Curtis RE, Linet MS, Morton LM. Acute leukemia incidence and patient survival among children and adults in the United States, 2001-2007. Blood. 2012, 119:34–43

5. Jabo B, Morgan JW, Martinez ME, Ghamsary M, Wieduwilt MJ. Sociodemographic disparities in chemotherapy and hematopoietic cell transplantation utilization among adult acute lymphoblastic and acute myeloid leukemia patients. PLoS One. 2017;12:e0174760. doi: 10.1371/journal.pone.0174760.
6. Kamath GR, Tremblay D, Coltoff A, Caro J, Lancman G, Bhalla S, Najfeld V, Mascarenhas J, Taioli E. Comapring the epidemiology, clinical characteristics and prognostic factor of acute myeloid leukemia with and without acute promyelocytic leukemia. Carcinogenesis, 2019, Jan 23, PMID: 30715157 DOI:10.1093/carcin/bgz014.
7. Breccia, M., et al. Early hemorrhagic death before starting therapy in acute promyelocytic leukemia: association with high WBC count, late diagnosis and delayed treatment initiation. Haematologica, 2010, 95:853-4.
8. Robak T, Wierzbowska A. Current and emerging therapies for acute myeloid leukemia. Clinical Therapeutics, 2009, 31:1346-2370
9. Calgarotto AK, Maso V, J.unior GC, Nowill AE, Filho PL, Vassallo J., Saad STO. Antitumor activities of quercetin and green tea in xenografts of human leukemia HL60 cells. Sci Rep. 2018, 8:3459.
10. Chabner BA. In: Goodman & Gilman's The Pharmacological Basis of Therapeutics. 11th Edition. Brunton LL, Lazo J.S, Parker KL, editors New York, 2006, 1257–1262 (McGraw-Hill).
11. Guérritte F. 2005. On: Anticancer Agents from Natural Products. Cragg GM, Kingston DGI, Newman DJ., editors Boca Raton, FL, 2005, 123–135 (CRC/Taylor & Francis).
12. Bellmunt J, Albanell H, Gallego OS, Ribas A, Vicente P, Carulla H, De Torres J, Morote J, Lopez M, Sole LA. Carboplatin, methotrexate, and vinblastine in patients with bladder cancer who were ineligible for cisplatin-based chemotherapy. Cancer, 1992, 70:1974-9.
13. Fraschini G, Yap HY, Hortobagyi GN, Buzdar A, Blumenschein G. Five-day continuous-infusion vinblastine in the treatment of breast cancer. Cancer, 1985, 56, 225-9.
14. Vainionpaa L, Kovala T, Tolonen U, Lanning M. Vincristine therapy for children with acute lymphoblastic leukemia impairs conduction in the entire peripheral nerve. Pediatric Neurol. 1995, 13, 314–8.
15. Varedi M, Ness KK, McKenna RF. Balance deficits in long-term pediatric ALL survivors. Oncotarget, 208, 9:32554-32555.
16. Torello CO. Reactive oxygen species production triggers green tea-induced anti-leukemic effects on acute promyelocytic leukemia model. Cancer Letters, 2017, 10, 116–126.
17. Hao Y., Zhang N, Wei N, Yin H, Zhang Y, Xu H, Zhou C, Doujie Li. Matrine induces apoptosis in acute myeloid leukemia cells by inhibiting the PI3K/Akt/mTOR signaling pathway. Oncol Lett, 2019; 18:2891-2896.
18. Roehrer S, Stork V, Ludwig C, Minceva M, Behr J. 2019. Analyzing bioactive effects of the minor hop component xanthohumol C on human breast cancer cells using quantitative proteomics. PLOS One, 2019. 14(3): e0213469.
19. Zanoli, P.; Zavatti, M. 2008. Pharmacognostic and pharmacological profile of Humulus lupulus L. J. Ethnopharmacol. 2008, 116:383–396.
20. Vogel S, Barbic M, Jürgenliemk G, Heilmann J. 2010. Synthesis, cytotoxicity, anti-oxidative and anti-inflammatory activity of chalcones and influence of A-ring modifications on the pharmacological effect. Eur J Med Chem. 2010 Jun; 45(6):2206-13.
21. Aydin T, Bayrak N, Baran E, Cakir A. Insecticidal effects of extracts of *Humulus lupulus (hops) L* cones and its principal component, xanthohumol. Bull Entomol Res, 2017, 10:543-549.
22. Lupinacci E, MeiJ.erink J, Vincken JP, Gabriele B, Gruppen H, Witkamp RF. Xanthohumol from hop *(Humulus lupulus L.)* is an efficient inhibitor of monocyte chemoattractant protein-1

and tumor necrosis factor-alpha release in LPS-stimulated RAW 264.7 mouse macrophages and U937 human monocytes. J.. Agric. Food Chem,.2009, 57, 7274–81.
23. Gerhauser, C, Alt A, Heiss E, Gamal-Eldeen, Klimo K, Knauft J, Neumann I, Scherf R, Frank N, Bartsch H, Becker H. Cancer chemopreventive activity of xanthohumol, a natural product derived from hop. Mold Cancer Therd, 2001, 1:959-969.
24. Dorn C, Kraus B, Motyl M, Weiss TS, Gehrig M, Schölmerich J., Heilmann J., Hellerbrand C. Xanthohumol, a chalcone derived from hops, inhibits hepatic inflammation and fibrosis. Mold Nutrd Food Resd, 2010, 54:S205-S213.
25. Legette LL, Luna AY, Reed RL, Miranda CL, Bobe G, Proteau RR, et al. 2013. Xanthohumol lowers body weight and fasting plasma glucose in obese male Zucker fa/fa rats. Phytochemistry, 2013, 91:236–41.
26. Gerhauser, C, Alt A, Heiss E, Gamal-Eldeen, Klimo K, Knauft J., Neumann I, Scherf R, Frank N, Bartsch H, Becker H. Cancer chemopreventive activity of xanthohumol, a natural product derived from hop. Mold Cancer Therd, 2002, 1:959-969.
27. Kunnimalaiyaan S, Trevino J., Tsai S, Gamblin TC, Kunnimalaiyaan M. 2015. Xanthohumol-mediated suppression of Notch1 signaling is associated with antitumor activity in human pancreatic cancer cells. Mol. Cancer Ther, 2015, 14:1395-403.
28. Sun Z, Zhou C, Liu F, Zhang W, Chen J., Pan Y, Ma L, Liu Q, Yang J., Wang Q. 2018. Inhibition of breast cancer cell survival by xanthohumol via modulation of the Notch signaling pathway in vivo and in vitro. Oncol. Lett, 2018, 15:908-916.
29. Venturelli S, Burkard M, Biendl M, Lauer UM, Frank J., Busch C. 2016. Prenylated chalcones and flavonoids for the prevention and treatment of cancer. Nutrition, 2018, 8:S0899-9007.
30. Slawinska-Brych A, Zdzisinska B, Dmoszynska-Graniczka M, Jeleniewicz W, Kurzepa J, Gagos M, Stepulak A. 2016. Xanthohumol inhibits the extracellular signal regulated (ERK) signaling pathway and suppresses cell growth of lung adenocarcinoma cells. Toxicology, 2016, 357:65-73.
31. Yong WK, Abd Malek SN. Xanthohumol induces growth inhibition and apoptosis in Ca Ski human cervical cancer cells. Evid Based Complement Alternat. Med. 2015, 921306.
32. Yong WK, Abd Malek SN. 2015. Xanthohumol induces growth inhibition and apoptosis in Ca Ski human cervical cancer cells. Evid Based Complement Alternat. Med. 2015, 921306.
33. Pacurari M, Qian Y, Porter DW, Wolfarth M, Wan Y, Luo D, Ding M, Castranova V, Guo N L. Multi-walled carbon nanotube-induced gene expression in the mouse lung: Association with lung pathology. Toxicol. Appl. Pharmacol, 2011, 255:18–31.
34. Pacurari M, Addison BJ, Bondalapati N, Wan YW, Luo D, Qian Y, Castranova V, Ivanov AV, Guo N. The microRNA-200 family targets multiple non-small cell lung cancer prognostic markers in H1299 cells and BEAS-2B cells. Intern J Oncology, 2013, 43:548-560.
35. Ramos NR, Co CC, Karp JE, Hourigan CS. Current approaches in the treatment of relapsed and refractory acute myeloid leukemia. J Clin Med, 2015, 4:665-695.
36. Corces-Zimmerman MR., Hong WJ., Weissman IL, Medeiros BC, MaJeti R. Preleukemic mutations in human acute myeloid leukemia affect epigenetic regulators and persist in remission. Proc Natl Acad Sci, USA, 2014, 111, 2548-2553.
37. Unnati S, Ripal S, SanJ.eev A, Nuyati A. 2013. Novel anticancer agents from plants. Chinese J. of Natural Medicines, 2013, 11:0016-0023.
38. Kumar A. 2016. Vincristine and vinblastine: a review. International J.ournal of Medicine and Pharmaceutical Sciences, 2016, 6:23-30.

39. Arimoto-Kobayashi S, Sugiyama C, Harada N, Takeuchi M, Takemura M, Hayatsu HJ. Inhibitory effects of beer and other alcoholic beverages on mutagenesis and DNA adduct formation induced by several carcinogens. Agric. Food Chem, 1999, 47:221–230.
40. Miranda CL, Stevens JF, Helmrich A, Henderson MC, Rodriguez RJ, Yang YH, Deinzer ML, Barnes DW, and Buhler DR. 1999. Antiproliferative and cytotoxic effects of prenylated flavonoids from hop (Humulus lupulus) in human cancer cell lines. Food Chem. Toxicol, 1999, 37:271 –285.
41Gerhauser C, Alt A, Heiss E, Gamal-Eldeen, Klimo K, Knauft J, Neumann I, Scherf R, Frank N, Bartsch H, Becker H. Cancer chemopreventive activity of xanthohumol, a natural product derived from hop. Mold Cancer Therd. 2002, 1:959-969.
42. Li Y, Wang K, Yin S, Zheng H, Min D. Xanthohumol inhibits proliferation of laryngeal squamous cell carcinoma. Oncol. Lett. 2016, 12:5289-5294.
43. Sun Z, Zhou C, Liu F, Zhang W, Chen J., Pan Y, Ma L, Liu Q, Yang J., Wang Q. 2018. Inhibition of breast cancer cell survival by xanthohumol via modulation of the Notch signaling pathway in vivo and in vitro. Oncol. Lett, 2018, 15;908-916.
44. Cao B., Chen H., Gao Y., Niu C., Zhang Y., Li L. 2015. CIP-36, a novel topoisomerase II-targeting agent, induces the apoptosis of multidrug-resistant cancer cells in vitro. Int J. Mol Med, 2015, 35;771–776.
45. Kaufmann SH, Desnoyers S, Ottaviano Y, Davidson NE, Poirier GG. Specific proteolytic cleavage of poly(ADP-ribose) polymerase: an early marker of chemotherapy-induced apoptosis. Cancer Res. 1993, 53:3976–3985.
46. Soldani C, Lazze MC, Bottone MG, Tgnon G, Biffigera M, Pellieciari CE, Scoassi AI. Poly(ADP-riobse) polymerase cleavage during apoptosis: When and Where. Experimental Cell Research, 2001, 269:193-201.
47. Harper JW, Adami GR, Wei N, Keyomarsi K, Elledge SJ. The p21 Cdk-interacting protein Cip1 is a potent inhibitor of G1 cyclin-dependent kinases. Cell, 1993, 75:805-16.
48. Sherr CJ, Roberts JM. CDK inhibitors: positive and negative regulators of G1-phase progression. Genes Dev, 1999, 13:1501–12.
49. Coqueret O. 2003. New roles for p21 and p27 cell-cycle inhibitors: a function for each cell compartment? Trends Cell Biol, 2003, 13:65-70.